

# 양자우물구조에 의한 태양전지 단락전류 증가 효과와 이차이온 질량분석법에 의한 원소 정량 분석

김정환<sup>†</sup>

세종대학교 에너지자원공학과  
(2019년 6월 4일 접수, 2019년 6월 7일 심사, 2019년 6월 12일 채택)

## Effect of Short Circuit Current Enhancement in Solar Cell by Quantum Well Structure and Quantitative Analysis of Elements Using Secondary Ion Mass Spectrometry

Junghwan Kim<sup>†</sup>

Department of Energy and Mineral Resources Engineering, Sejong University, Seoul 05006, Republic of Korea  
(Received June 4, 2019; Revised June 7, 2019; Accepted June 12, 2019)

### 초 록

GaInP/GaAs 양자우물(quantum well)구조를 N-AlGaInP/p-GaInP 이중 접합구조 태양전지에 도입하여 그 특성을 조사하고 양자우물구조가 없는 태양전지와 비교하였다. 에피층은 (100)평면이 (111)A 방향으로 6° 기울어진 p-GaAs 기판 위에 성장하였다. 태양전지 박막구조는 두께 400 nm의 N-AlGaInP 층에 590 nm의 p-GaInP와 210 nm의 GaInP/GaAs 양자우물 구조(10 nm GaInP/5 nm GaAs의 14겹 구조)가 도입된 양자우물 태양전지 구조와 800 nm의 p-GaInP의 단일이종접합 구조로 이루어진다. 측정결과 1 × 1 mm<sup>2</sup>의 태양전지에서 단락전류밀도( $J_{sc}$ )는 양자우물구조가 도입된 태양전지에서는 9.61 mA/cm<sup>2</sup>, 양자우물 구조가 없는 태양전지에서는 7.06 mA/cm<sup>2</sup>가 각각 측정되었다. 이차이온질량 분석법(SIMS)과 외부양자효율(external quantum efficiency) 측정을 통하여 단락전류 증가에 의한 효율증가가 흡수 스펙트럼의 확대가 아닌 양자우물에 의한 carrier 재결합의 억제에 의한 효과임을 확인하였다.

### Abstract

Characteristics of solar cells employing a lattice matched GaInP/GaAs quantum well (QW) structure in a single N-AlGaInP/p-InGaP heterojunction (HJ) were investigated and compared to those of solar cells without QW structure. The epitaxial layers were grown on a p-GaAs substrate with 6° off the (100) plane toward the <111>A. The heterojunction of solar cell consisted of a 400 nm N-AlGaInP, a 590 nm p-GaInP and 14 periods of a 10 nm GaInP/5 nm GaAs for QW structure and a 800 nm p-GaInP for the HJ structure (control cell). The solar cells were characterized after the anti-reflection coating. The short-circuit current density for 1 × 1 mm<sup>2</sup> area was 9.61 mA/cm<sup>2</sup> for the solar cell with QW structure while 7.06 mA/cm<sup>2</sup> for HJ control cells. Secondary ion mass spectrometry and external quantum efficiency results suggested that the significant enhancement of  $J_{sc}$  and EQE was caused by the suppression of recombination by QW structure.

**Keywords:** Heterojunction structure, Quantum well, Solar cells, Secondary ion mass spectrometry, Carrier recombination

## 1. Introduction

To achieve better cost-effectiveness, several approaches have been explored. The approaches are mainly divided into two categories: improving energy conversion efficiencies of solar cells and reducing manufacturing cost. The energy conversion efficiency can be accomplished

by either improving performance characteristics of solar cells such as short circuit current, open circuit voltage, and shunt resistance or extending the absorption spectrum of solar cells. Various efforts have been made to improve the spectral response of photovoltaic cells. The highest current conversion efficiency has achieved in III-V compound semiconductor multi-junction (MJ) photovoltaic (PV) cells in which several pn junctions with different bandgap semiconductor materials are stacked to cover different spectrum[1,2]. As a different approach, quantum wells (QWs)[3] or quantum dots (QDs)[4] having different bandgaps were inserted into the absorption layers. Solar cell structures such as strain-balanced InGaAsP/GaInP QW structure[5,6], InGaAs/GaAsP QW structure employed in GaInP/GaAs tandem solar cell[7] and

<sup>†</sup> Corresponding Author: Sejong University,  
Department of Energy and Mineral Resources Engineering, Seoul 05006,  
Republic of Korea  
Tel: +82-2-3408-3978 e-mail: junghwan@sejong.ac.kr

GaSb/InGaAs QD and QW hybrid structure[8] have been explored. The open circuit voltage ( $V_{oc}$ ) is determined by smaller energy bandgap ( $E_g$ ) material when two different bandgap materials are used. The  $V_{oc}$  approximately amounts to 0.6 of the smaller energy bandgap ( $E_g$ ) material. However, if QW or QD materials are inserted in the absorption layer of the PV cell, it is possible to increase the absorption spectrum without significant decrease in  $V_{oc}$ . The number of QW needs to be optimized because the  $V_{oc}$  decreases as the QW layers increase[9]. In our previous report, we demonstrated  $N$ -AlGaInP/ $p$ -GaInP single heterojunction structure solar cells[10]. Since the bandgap energy of the AlGaInP is 2.2 eV ( $\lambda_{AlGaInP} = 560$  nm) and the bandgap energy of the GaInP layer is 1.85 eV ( $\lambda_{GaInP} = 670$  nm), no light absorption occurs above the wavelength 670 nm. To extend the solar absorption spectrum edge, a semiconductor with  $E_g$  less than 1.85 eV needs to be employed. In this report, we have proposed a simple GaInP/GaAs QW heterojunction structure inserted in  $N$ -AlGaInP/ $p$ -GaInP heterojunction structure because the QW layers are easily lattice matched to GaAs substrate. The characteristics of the QW structure solar cells were compared with single heterojunction structure solar cells. A significant enhancement in both short circuit current density ( $J_{sc}$ ) and external quantum efficiency (EQE) were observed without absorption spectrum extension while the  $V_{oc}$  was reduced slightly from 1.42 V to 1.40 V. There have been reports to suppression of recombination to increase  $J_{sc}$ [11-13] This result is different with previous works in QW structures report because the previous reports by other groups achieved the enhancement in  $J_{sc}$  with a slight increase in absorption spectrum due to insertion of QW layers. This result suggests that  $J_{sc}$  can be improved significantly without extending absorption spectrum. The suppression of recombination. If it is verified that the insertion of the QW structures suppresses the carrier recombination and thus results in better performance, it can be used in optical or electrical devices such as photodetectors, high speed transistors, and solar cells.

## 2. Experiment

The  $N$ -AlGaInP/ $p$ -GaInP single heterojunction solar cell structures were grown on  $p$ -GaAs substrates by metalorganic vapor phase epitaxy (MOCVD) in the Korea Advanced Nano-fabrication Center. The  $p$ -GaAs substrates were cut  $6^\circ$  off the (100) plane toward the  $\langle 111 \rangle_A$  direction. The epitaxial layer structures consist of a 200 nm  $p$ -GaAs contact layer, a 50 nm  $p$ -AlInP back surface field layer, a 590 nm  $p$ -GaInP ( $E_g = 1.85$  eV) and 14 periods of a 10 nm  $p$ -GaInP/5 nm  $p$ -GaAs for QW structure or 800 nm  $p$ -GaInP for single heterojunction (HJ) structure (control cell), and an 400 nm  $N$ -AlGaInP ( $E_g = 2.2$  eV) emitter layer followed by a  $N$ -AlInP window layer ( $E_g = 2.36$  eV), and  $n$ -GaAs contact layer on top. All epilayers were lattice-matched to GaAs. The epitaxial layer structures were shown in Figure 1 (a) for QW structure and Figure 1 (b) for single HJ structure.

For backside  $p$ -metalization, Ti/Pt/Au were deposited on the back side of a GaAs substrate after a front side protective photoresist (PR) was applied. The thicknesses of the  $p$ -metals are 20 nm/20 nm/460 nm, respectively. For the front side  $n$ -metallization, grid patterns were

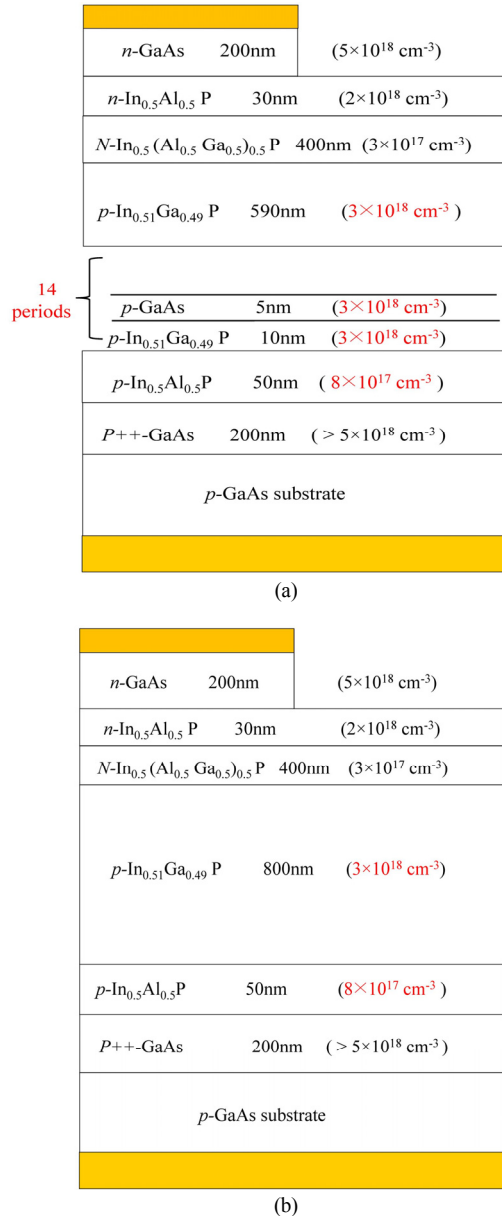


**Figure 1. Schematic epitaxial layer structures of (a)  $N$ -AlGaInP/ $p$ -GaInP/ $p$ -GaAs QW structure, (b) single  $N$ -AlGaInP/ $p$ -GaInP heterojunction (control cell).**

formed by standard photolithography.  $n$ -metal contacts of AuGe/Ni/Au (80 nm/80 nm/400 nm thickness) were deposited and lifted off. The  $n$ -GaAs contact layer was etched to avoid unintended light absorption at the top contact layer and the mesas for active solar cell areas were formed by etching down to the GaAs substrate layer. Finally, ZnS/MgF<sub>2</sub> layers for anti-reflection coating were deposited.

## 3. Results and Discussion

### 3.1. Current density-voltage characteristics

The current density-voltage ( $J$ - $V$ ) characteristics of PV cells under a 1-sun illumination condition are shown in Figure 2. The measurement

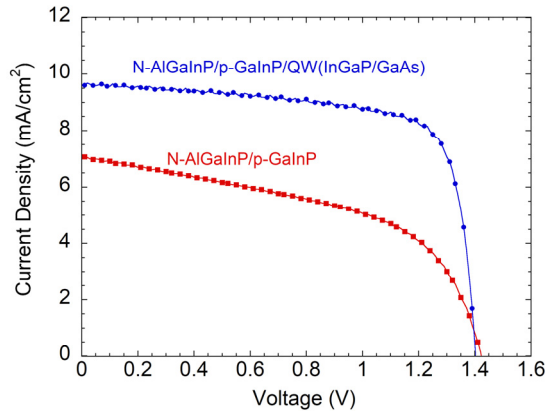


Figure 2. Current density-voltage ( $J$ - $V$ ) characteristics of PV cells under a 1-sun illumination condition from  $1 \text{ mm} \times 1 \text{ mm}$  area devices having  $20 \text{ }\mu\text{m}$  width and  $174 \text{ }\mu\text{m}$  spacing line grids.

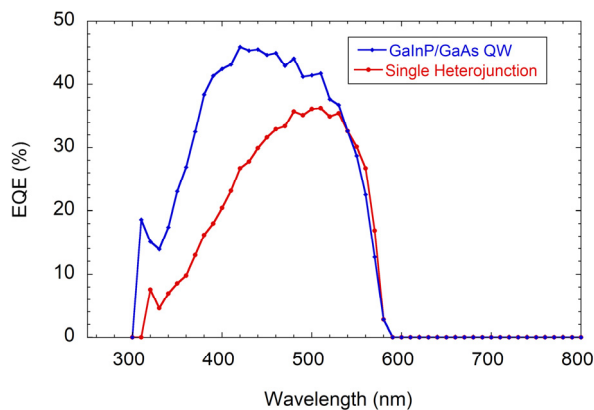


Figure 3. Comparison of external quantum efficiencies for  $5 \text{ mm} \times 5 \text{ mm}$  area solar cells.

results were obtained from  $1 \text{ mm} \times 1 \text{ mm}$  area devices with  $20 \text{ }\mu\text{m}$  width and  $174 \text{ }\mu\text{m}$  spacing line grids. The short-circuit current densities ( $J_{sc}$ s) were  $9.61 \text{ mA/cm}^2$  for QW structure and  $7.06 \text{ mA/cm}^2$  for single HJ control cell, respectively. The  $J_{sc}$  was increased 36% in the solar cell employing QW structure. The open-circuit voltages ( $V_{oc}$ s) were  $1.40 \text{ V}$  for QW structure and  $1.42 \text{ V}$  for single HJ structure. The  $V_{oc}$  was slightly decreased and the reduction was less than 2% in the structure employing a  $210 \text{ nm}$  thick GaInP/GaAs QW (14 periods). Considering the fact that the bandgap of GaAs is  $1.42 \text{ eV}$  and the  $V_{oc}$  of GaAs solar cell has the value around  $1.02 \text{ V}$ [14], the introducing GaAs in QW indicates a relatively small decrease of  $V_{oc}$  as anticipated. In addition to the increased  $J_{sc}$ , the shunt resistance of QW structure solar cell is higher than that of single HJ solar cell. The efficiency of QW structure is 10 % and the efficiency of single HJ control cell is 5.2%. By introducing a QW structure into AlGaInP/GaInP HJ structure solar cell, the overall efficiency was almost doubled.

### 3.2. External quantum efficiency

External quantum efficiencies (EQEs) were measured to obtain the absorption spectral response and the measured EQEs are shown in

Figure 3. The results were obtained from  $5 \text{ mm} \times 5 \text{ mm}$  area cells without ARC. The maximum EQE was measured 36.3% at  $510 \text{ nm}$  for single HJ control cell and 46% at  $420 \text{ nm}$  for QW structure cell, respectively. The absorption edges of both solar cells were  $580 \text{ nm}$  which corresponds to bandgap energy of  $2.16 \text{ eV}$ . The QW structure showed higher EQE than the single HJ structure, but no absorption occurred in GaInP/GaAs QW layer. Preliminarily, we speculated that the  $J_{sc}$  improvement was attributed to the absorption spectrum extension by GaInP/GaAs QW layer. However, the measured EQE data indicated that there is no enhancement of the absorption edge due to the QW layer. Since the cause of  $J_{sc}$  enhancement in QW structure was different from our assumption, it is imperative to find out the explanation for the improvement of the  $J_{sc}$ .

### 3.3. Secondary ion mass spectrometry depth profile

From EQE data, it was observed that the solar spectrum above the wavelength longer than  $580 \text{ nm}$  were not absorbed at all. Therefore, we need to verify whether  $p$ -GaInP/ $p$ -GaAs QW layers were grown in epitaxial layers as we designed. A secondary ion mass spectrometry (SIMS) was used for depth profiling of both epilayers. Figure 4 illustrates the SIMS depth profiles of the QW structure and HJ control structure. Two structures are identical except the  $210 \text{ nm}$  thick 14 periods of  $p$ -GaInP/ $p$ -GaAs QW layer. The most distinct difference in compositional element between both epitaxial layers is Arsenic in QW structure as shown in Figure 4 (a), because QW structure contains GaAs whereas HJ control structure consists of GaInP only. The arsenic content was clearly observed only in QW structure. For Al, both structures showed high contents in  $N$ -AlGaInP layers and abruptly decreased in  $p$ -GaInP layer in a depth of  $800 \text{ nm}$ . As the bandgap energies of the absorption edges were measured  $2.16 \text{ eV}$  in both structures, which corresponds to the bandgap of  $N$ -AlGaInP, we suspected that the  $p$ -GaInP layers ( $E_g = 1.85 \text{ eV}$ ) were not grown appropriately. However, the Al contents indicated that  $p$ -GaInP layers were formed correctly as designed. According to the depth profiles shown in Figure 4 (c)~(e), Gallium (Ga), phosphorus (P), and indium (In) contents also indicated that GaInP/GaAs QW layers were formed in the region from  $1,200 \text{ nm}$  to  $1,450 \text{ nm}$  depth. Oxygen atoms were known to be a non-radiative recombination center. The O concentration is almost same in both epitaxial layer structures.

From the EQE, we can see that light was absorbed only in the AlGaInP layers from  $250 \text{ nm}$  to  $750 \text{ nm}$  for both solar cells. SIMS depth profile indicated that the epitaxial layers of both solar cells are different only in the QW layers, which means that the thicknesses of epilayers, the material composition, and oxygen concentration cannot be a factor to generate the significant difference in the performance of the solar cells. However, the solar cell with QW structure showed 36% enhancement in  $J_{sc}$ . These results suggested that recombination during carrier transportation was suppressed by QW structure and thus the conversion efficiency was improved significantly. Increased efficiency through the suppression of recombination has been reported in nano-structured Si solar cells[15]. Our result is worth noting because the improvement in  $J_{sc}$  can be achieved without an extension of the response

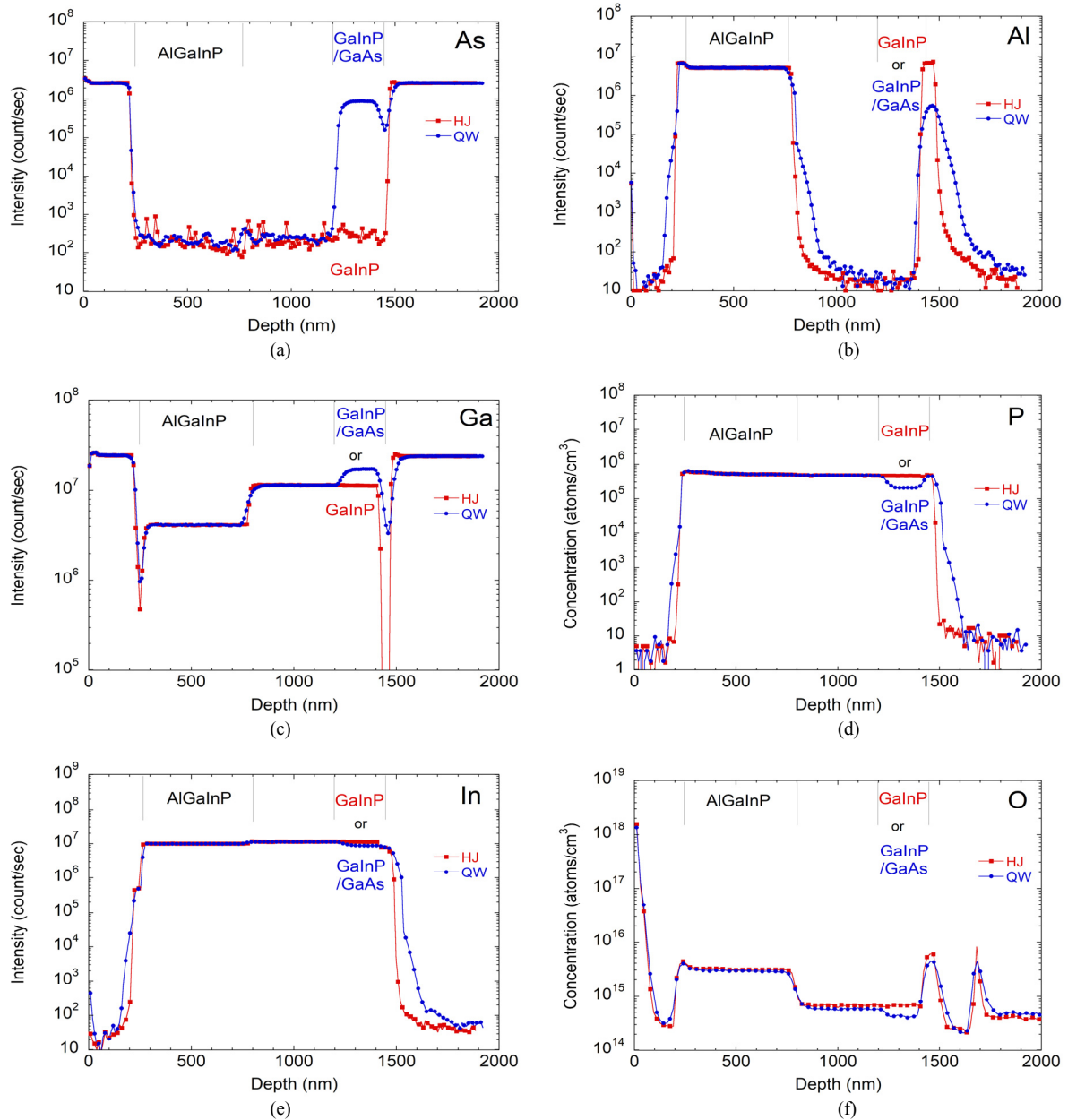


Figure 4. SIMS depth profiles of (a) arsenic, (b) aluminum, (c) gallium, (d) phosphorus, (e) indium, (f) oxygen concentration for both solar cells.

spectrum and the QW structure insertion in epilayer[16]. This indicate that inserting QW structure can improve carrier transport and thus results in conversion efficiency even without the absorption spectrum enhancement. There have been several theoretical report regarding current transport in QW structures[17,18]. Further investigation is required to explain more specific in photocurrent collection process in the QW structure.

#### 4. Conclusion

The characteristics of solar cells employing GaInP/GaAs QW structure in a single AlGaInP/InGaP HJ structure were compared with solar cells having single AlGaInP/InGaP HJ structure without QW layer. The

short-circuit current density was increased by 36% in the solar cell with the QW structure. In addition to the enhancement of  $J_{sc}$ , the shunt resistance improvement resulted in a significant increase in the conversion efficiency from 5.2% to 10%. The EQE data show that the absorption by the light above a wavelength of 580 nm did not occur in both solar cell structures. SIMS depth profile data indicated that the thicknesses of the both grown epilayers were identical except the QW layer. Since the *p*-GaInP/QW layers (QW structure) or the *p*-GaInP layer (single HJ structure) worked only for carrier transportation, it can be concluded that photogenerated carriers are collected more efficiently in QW structure. The high collection efficiency of photogenerated carriers is attributed to the suppression of recombination due to the existence of QW layers.

## Acknowledgment

This research was supported by Nano-Material Technology Development Program through the National Research Foundation of Korea (NRF) funded by the Ministry of Science, ICT and Future Planning (2009-0082580).

## References

1. R. M. France, J. F. Geisz, I. Garcia, M. A. Steiner, W. E. McMahon, D. J. Friedman, T. E. Moriarty, C. Osterwald, J. Scott Ward, A. Duda, M. Young, and W. J. Olavarria, Quadruple-junction inverted metamorphic concentrator devices, *IEEE J. Photovolt.*, **5**(1), 432-437 (2015).
2. Y. Jeong, D.-W. Park, J. K. Lee, and J. Lee, III-V tandem,  $\text{CuInGa}(\text{S,Se})_2$ , and  $\text{Cu}_2\text{ZnSn}(\text{S,Se})_4$  compound semiconductor thin film solar cells, *Appl. Chem. Eng.*, **26**(5), 526-532 (2015).
3. M. Mazzer, K. W. J. Barnham, I. M. Ballard, A. Bessiere, A. Ioannides, D. C. Johnson, M. C. Lynch, T. N. D. Tibbits, J. S. Roberts, G. Hill, and C. Calder, Progress in quantum well solar cells, *Thin Solid Films*, **511**, 76-83 (2006).
4. K. A. Sablon, J. W. Little, V. Mitin, A. Sergeev, N. Vagidov, and K. Reinhardt, Strong enhancement of solar cell efficiency due to quantum dots with built-in charge, *Nano Lett.*, **11**(6), 2311-2317 (2011).
5. I. E. Hashem, C. Z. Carlin, B. G. Hagar, P. C. Colter, and S. M. Bedair, InGaP-based quantum well solar cells: Growth, structural design, and photovoltaic properties, *J. Appl. Phys.*, **119**(9), 095706 (2016).
6. I. E. H. Sayed, C. Z. Carlin, B. G. Hagar, P. C. Colter, and S. M. Bedair, Strain-balanced InGaAsP/GaInP multiple quantum well solar cells with a tunable bandgap (1.65-1.82 eV), *IEEE J. Photovolt.*, **6**(4), 997-1003 (2016).
7. G. K. Bradshaw, J. P. Samberg, C. Z. Carlin, P. C. Colter, K. M. Edmondson, W. Hong, C. Fetzer, N. Karam, and S. M. Bedair, GaInP/GaAs tandem solar cells with InGaAs/GaAsP multiple quantum wells, *IEEE J. Photovolt.*, **4**(2), 614-619 (2014).
8. R. B. Laghumavarapu, B. L. Liang, Z. S. Bittner, T. S. Navruz, S. M. Hubbard, A. Norman, and D. L. Huffaker, GaSb/InGaAs quantum dot - well hybrid structure active regions in solar cells, *Sol. Energy Mater. Sol. Cells*, **114**, 165-171 (2013).
9. S. A. Mintairov, N. A. Kalyuzhnyy, M. V. Maximov, A. M. Nadochiy, and A. E. Zhukov, InGaAs quantum well-dots based GaAs subcell with enhanced photocurrent for multijunction GaInP/GaAs/Ge solar cells, *Semicond. Sci. Technol.*, **32**(1), 015006 (2017).
10. J. Kim and H.-B. Shin, Effect of substrate off-orientation on the characteristics of GaInP/AlGaInP single heterojunction solar cells, *Korean J. Chem. Eng.*, **36**(2), 305-311 (2019).
11. F. Wu, H. Lin, Z. H. Yang, M. D. Liao, Z. L. Wang, Z. P. Li, P. Q. Gao, J. C. Ye, and W. Z. Shen, Suppression of surface and Auger recombination by formation and control of radial junction in silicon microwire solar cells, *Nano Energy*, **58**, 817-824 (2019).
12. K. Toprasertpong, T. Inoue, Y. Nakano, and M. Sugiyama, Investigation and modeling of photocurrent collection process in multiple quantum well solar cells, *Sol. Energy Mater. Sol. Cells*, **174**, 146-156 (2018).
13. M. C. Lynch, I. M. Ballard, D. B. Bushnell, J. P. Connolly, D. C. Johnson, T. N. D. Tibbits, K. W. J. Barnham, N. J. Ekins-Daukes, J. S. Roberts, G. Hill, R. Airey, and M. Mazzer, Spectral response and I-V characteristics of large well number multi quantum well solar cells, *J. Mater. Sci.*, **40**(6), 1445-1449 (2005).
14. G. J. Bauhuis, P. Mulder, E. J. Haverkamp, J. C. C. M. Huijben, and J. J. Schermer, 26.1% thin-film GaAs solar cell using epitaxial lift-off, *Sol. Energy Mater. Sol. Cells*, **93**(9), 1488-1491 (2009).
15. S. Zhong, Z. Huang, X. Lin, Y. Zeng, Y. Ma, and W. Shen, High-efficiency nanostructured silicon solar cells on a large scale realized through the suppression of recombination channels, *Adv. Mater.*, **27**(3), 555-561 (2015).
16. J. Nelson, J. Barnes, N. Ekins-Daukes, B. Kluitinger, E. Tsui, K. Barnham, C. T. Foxon, T. Cheng, and J. S. Roberts, Observation of suppressed radiative recombination in single quantum well p-i-n photodiodes, *J. Appl. Phys.*, **82**(12), 6240-6246 (1997).
17. S. C. McFarlane, J. Barnes, K. W. J. Barnham, E. S. M. Tsui, C. Button, and J. S. Roberts, Space charge effects in carrier escape from single quantum well structures, *J. Appl. Phys.*, **86**(9), 5109-5115 (1999).
18. A. Luque, E. Antolín, P. G. Linares, I. Ramiro, A. Mellor, I. Tobias, and A. Martí, Interband optical absorption in quantum well solar-cells, *Sol. Energy Mater. Sol. Cells*, **112**, 20-26 (2013).